Received: 7 April 2021 | Revised: 17 May 2021 | Accepted: 17 May 2021

DOI: 10.1002/psc.3355

RESEARCH ARTICLE

Journal of PeptideScience WILEY

Transmembrane β-peptide helices as molecular rulers at the membrane surface

Martin Kloos[1] | Akshita Sharma[2] | Jörg Enderlein[2,3] | Ulf Diederichsen[1]

[1]Institut für Organische und Biomolekulare Chemie, Georg-August-Universität Göttingen, Göttingen, Germany

[2]III. Physikalisches Institut—Biophysik, Georg-August-Universität Göttingen, Göttingen, Germany

[3]Cluster of Excellence "Multiscale Bioimaging: from Molecular Machines to Networks of Excitable Cells" (MBExC), Georg-August-Universität Göttingen, Göttingen, Germany

Correspondence
Ulf Diederichsen, Institut für Organische und Biomolekulare Chemie, Georg-August-Universität Göttingen, Tammannstraße 2, 37077 Göttingen, Germany.
Email: udieder@gwdg.de

Funding information
Deutsche Forschungsgemeinschaft, Grant/Award Numbers: EXC 2067/1-390729940, SFB 803

β-Peptides are known to form 14-helices with high conformational rigidity, helical persistence length, and well-defined spacing and orientation regularity of amino acid side chains. Therefore, β-peptides are well suited to serve as backbone structures for molecular rulers. On the one hand, they can be functionalized in a site-specific manner with molecular probes or fluorophores, and on the other hand, the β-peptide helices can be recognized and anchored in a biological environment of interest. In this study, the β-peptide helices were anchored in lipid bilayer membranes, and the helices were elongated in the outer membrane environment. The distances of the covalently bound probes to the membrane surface were determined using graphene-induced energy transfer (GIET) spectroscopy, a method based on the distance-dependent quenching of a fluorescent molecule by a nearby single graphene sheet. As a proof of principle, the predicted distances were determined for two fluorophores bound to the membrane-anchored β-peptide molecular ruler.

KEYWORDS
grapheneMIET, molecular ruler, sensor, transmembrane domain, β-peptide

1 | INTRODUCTION

Distance determination on the nanometer scale and spatially defined placement of probes is of importance in the study of biochemical mechanisms in model systems and in cells.[1,2] One possibility for spatially defined alignment of probes is provided by molecular rulers, which address defined distances by their topological rigidity.[3,4] By defined interaction and anchoring of these molecular rulers in the biochemical contexts, distances can be read out physico-chemically on the basis of probe molecules. Common methods for analyzing nanoscale distances include X-ray scattering,[5] NMR and EPR spectroscopy,[6] and fluorescence measurements.[7]

Here, we describe the application of the molecular ruler concept to the addressability of defined distances from the surface of a lipid bilayer membrane. The need for a membrane-proximal molecular ruler is due to the measurement of, for example, proton or calcium ion gradients along the membrane surface, which, together with the proximal environment, drive biochemical processes such as SNARE protein-mediated membrane fusion.[8] Molecular rulers that define the distance from the membrane surface enable distance-defined placement of sensors to study the membrane-proximal environment. Long-term goals include analysis of increased acidity on the surface of diseased tissue as a function of membrane distance[9] or flux of protons and calcium ions along the membrane surface.[10]

DNA double strands are ideally suited as a molecular ruler given the repetitive rise of the double-stranded helix, linear highly rigid secondary structure, and options for functionalization. Therefore, DNA double strands serve as a prominent topology for a molecular ruler.[11] Examples for their application are the determination of point-

Dedicated to the memory of Klaus Hafner.

to-point distances in solution by inserting two gold probes and performing solution X-ray scattering[12] and the tandem SH2 domain that was measured with self-assembled, bivalent DNA-peptide conjugates.[3] An alternative biooligomer to DNA and comparable in terms of helix persistence are β-peptide helices.[13] In addition to the formation of long and rigid helices, β-peptides can be functionalized at the amino acid side chains in regular intervals; the polarity and the possible interactions of the β-peptide helix are defined by choosing the proper sequence. In general, β-peptides are derived from α-amino acids containing an additional methylene unit compared with α-amino acids.[14–21] Depending on the position and configuration of the side chains, β-peptides yield well-defined secondary structures, with the 14-helix secondary structure being particularly valuable for the molecular ruler approach, because three amino acids per turn yield a conformationally highly stable helix with long persistence length and a 1.56 Å rise per residue.

In previous studies, we have established the β-peptide 14-helices with nonpolar homovaline sequences as transmembrane domains in model lipid bilayers.[17–19] There is clear evidence for the β-peptide helices being incorporated into the lipid bilayer by spanning the membrane and anchoring well with flanking homotryptophane side chains recognized by the lipid head group area. The 14-helix conformation remains intact even when incorporated into the membranes. Finally, we also have evidence that the transmembrane segments of peptides **P1** and **P2** (Figure 1) were incorporated into a large unilamellar vesicles (LUVs) of DOPC, which have a bilayer thickness of 27–29 Å with a tilt angle of 16°. This tilt angle of transmembrane β-peptides upon reconstitution into a DOPC membrane was determined by X-ray studies with labeled heavy atoms[19] and EPR spectroscopy.[22,23]

The concept of a β-peptide 14-helical transmembrane molecular ruler is based on the highly stable helix conformation even when the β-peptide sequence is extended beyond the membrane portion. While in general the conformational stability of a β-peptide 14-helix in water is limited[24] it needs to be stabilized by trans-1-(benzyloxycarbonyl-amino)-cyclohexyl-2-carboxylic acid (ACHC)[25] or salt bridges.[26,27] For this proof-of-concept study, we are confident that extension of the β-peptide into the water environment will keep the 14-helix conformation largely intact. This assumption is based on the elongating effect of the transmembrane 14-helix on the extramembrane helical conformation and on CD spectra obtained for the β-peptide H-(β^3hLys-β^3hVal)$_4$-β^3hLys-NH$_2$ in water, indicating a high 14-helix secondary structure content.[28]

As a proof of concept, we synthesized two transmembrane β-peptides **P1** and **P2** differing in length of the extramembrane part and attached an Atto643 fluorophore at the respective *N*-terminus (Figure 2), both being characterized by mass spectrometry and CD spectroscopy. After membrane incorporation, the distance of the respective fluorophore from the membrane was determined with graphene-induced energy transfer (GIET). As expected, distances of 5.5 and 6.2 nm were measured for the fluorophores with respect to the graphene-coated glass underlying the lipid bilayer.

2 | MATERIALS AND METHODS

2.1 | General

The NovaPEG Rink Amide resin LL (0.20 mmol/g) was obtained from Novabiochem (Darmstadt, Germany); 1-hydroxy-7-azabenzotriazol (HOAt) was provided by GL Biochem (Shanghai, China); 2-(7-aza-1*H*-benzotriazole-1-yl)-1,1,3,3-tetramethyluronium hexafluorophosphate (HATU) and 1,1,1,3,3,3-hexafluoro-2-propanol (HFIP) were purchased from Fluorochem Ltd (Hadfield, UK); piperidine, *N*-methyl-2-pyrrolidone (NMP), *N*,*N*-diisopropylethylamine (DIPEA), acetic acid anhydride (Ac_2O), and trifluoroacetic acid (TFA) were purchased from Carl Roth GmbH (Karlsruhe, Germany); 1,8-diazabicyclo[5.4.0] undec-7-en (DBU) was obtained from Carbolution Chemicals GmbH (St. Ingbert, Germany); *N*,*N*-dimethyformamide (DMF) and methanol (MeOH) high-performance liquid chromatography (HPLC) grade were purchased from Fluka (Taufkirchen, Germany); and triisopropylsilane (TIS) was obtained from TCI (Tokyo, Japan). Ultra-pure water was obtained by using the purification system arium® mini (Sartorius AG, Göttingen, Germany). Lipids were purchased from Avanti Polar Lipids (Alabama, USA), and atto-fluorophores were provided by ATTO-TEC GmbH (Siegen, Germany).

2.2 | Synthesis of β^3-peptides P1 and P2

Microwave-assisted solid-phase peptide synthesis was performed with a Discover microwave device in a Becton–Dickinson

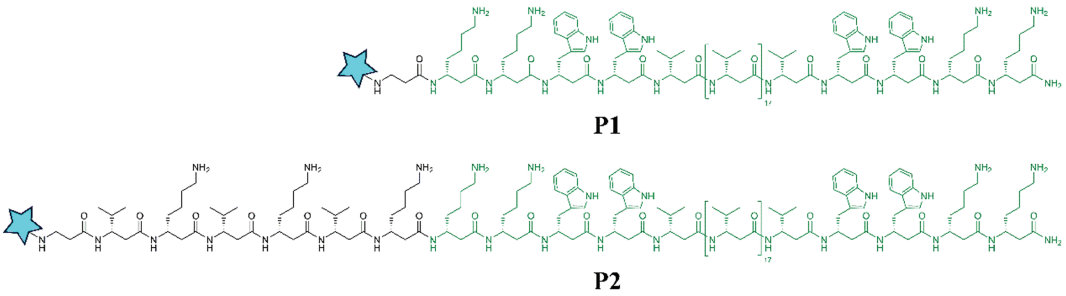

FIGURE 1 Chemical structures of synthesized transmembrane β-peptides P1 and P2. Transmembrane regions are depicted in green, and the attached Atto643 is shown in blue

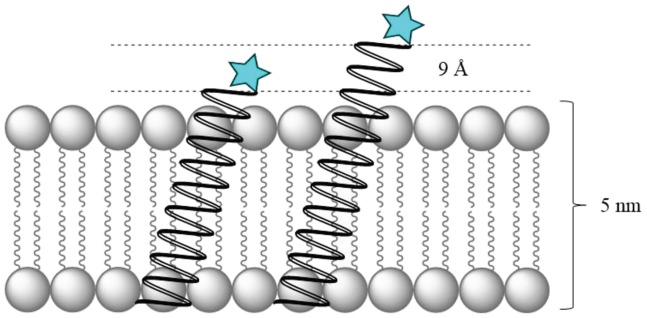

FIGURE 2 Model of the transmembrane β-peptides **P1** and **P2** differing in the helix extension in the outer membrane area leading to defined distances of the fluorophore (blue star) to the membrane surface

(BD) syringe using a PE filter.[18] All peptides were synthesized on a NovaPEG Rink Amide resin with low occupancy (0.20 mmol/g). Prior to use, resins were swollen in DMF for 2 h at room temperature. For efficient removal of *N*-terminal Fmoc-protecting groups, two microwave-assisted deprotection steps (50 W, 65°C, 30 s and 25 W, 65°C, 3 min) were carried out using DBU/piperidine/NMP (1:20:79, *v*/*v*/*v*). After washing with MeOH and DMF, respective amino acids (5.00 eq) were dissolved in a solution of 0.5 M HOAt (5.00 eq) and 0.5 M HATU (4.90 eq) in DMF, followed by further activation via 2.0 M DIPEA (10.0 eq) in DMF. Coupling steps (30 W, 65°C, 15 min) were performed twice with subsequent washing steps each. Remaining amino functions were capped with Ac_2O/NMP (1:4, *v*/*v*). After completion of the final peptide sequences, final Fmoc deprotection was performed. *N*-Terminal Atto643 labeling was achieved by dissolving the NHS ester (0.81 eq) in dry DMSO (400 μl), adding the mixture and DIPEA (4.00 eq) to the resin. The labeling reaction was performed microwave assisted (10 W, 37°C, 2 h) and then shaken at 37°C overnight. The resin was washed thoroughly with DMF, MeOH, DCM, and diethyl ether. After drying the resin under reduced pressure, removal of all protecting groups and cleavage of the peptide from the resin was carried out with TFA/H_2O/TIS (95:2.5:2.5, *v*/*v*/*v*) for 2 h at room temperature. Drying in a nitrogen stream and precipitation in cold diethyl ether led to the crude peptide which was further purified via HPLC in a purity > 90%.

P1. ESI-MS (*m*/*z*): 1476.58 $[M + 3H]^{3+}$, 1491.27 $[M + 3H + CO_2]^{3+}$, 1506.21 $[M + 3H + 2CO_2]^{3+}$. HPLC (gradient: 80% to 100% B in 30 min at 40°C): $t_R = 34.5$ min.

P2. ESI-MS (*m*/*z*): 1731.67 $[M + 3H]^{3+}$, 1299.25 $[M + 4H]^{4+}$, 1039.5 $[M + 5H]^{5+}$, 866.5 $[M + 6H]^{6+}$. HPLC (gradient: 70% to 100% B in 30 min): $t_R = 33.0$ min.

2.3 | Bilayer preparation

Giant unilamellar vesicles (GUVs) were obtained by drying 60 μl of peptide/lipid mixture (59 μl of 10-mg/ml DOPC in chloroform, P/L 1:25000) at 30°C on an aluminum electrode under reduced pressure. The resulting lipid film was rehydrated with 300 mM sucrose solution (500 μl) and treated with 15-Hz alternating current for 3 h with a peak-to-peak voltage of 1.6 V. Afterwards, an 8-Hz current was applied for 30 min. The resulting GUV solution was diluted with PBS buffer (500 μl). GUVs were spread by 30-fold dilution of the vesicle solution and adding it to a graphene substrate (Graphene Supermarket, New York, USA). After 1 h, the resulting bilayer was washed carefully with PBS buffer.

2.4 | GIET spectroscopy

GIET spectroscopy[29] relies on the distance-dependent quenching of a fluorescent molecule by a nearby single sheet of graphene.[30] In this process, the excited state energy of a fluorescent molecule is coupled, via electrodynamic near-field interaction, into excitons in graphene, which leads to a well-defined monotonous relationship between molecule–graphene distance and fluorescence lifetime (see also Section 3). This is similar to more conventional Förster resonance energy transfer where the role of graphene is taken by a suitable acceptor molecule. The lifetime–distance relationship is calculated by solving Maxwell's equations for an electric dipole emitter in the vicinity of a graphene-covered glass substrate (for details see Ghosh et al.[29]). These calculations provide the radiative emission power $S(\alpha, z_0)$ of the dipole as a function of its distance z_0 from the surface, and of its orientation α. Knowing this function, the measurable fluorescence lifetime $\tau_f(\alpha, z_0)$ is then given by the following expression:

$$\frac{\tau_f(\alpha, z_0)}{\tau_0} = \frac{S_0}{\phi S(\alpha, z_0) + (1-\phi)S_0}, \quad (1)$$

where τ_0 is the free-space fluorescence lifetime (no graphene-covered glass substrate), ϕ is the fluorescence quantum yield (QY), and S_0 is the radiative emission rate of an ideal electric dipole emitter in free space. The latter is given by $S_0 = cnk_0^4p^2/3$, where c denotes the vacuum speed of light, n is the refractive index of the surrounding medium, $k_0 = 2\pi/\lambda$ is the vacuum wave vector for light of wavelength λ, and p is the oscillator's dipole moment amplitude. Please note that the latter is dropping out from Equation (1) because $S(\alpha, z_0)$ does also linearly depend on p. One important property of $\tau_f(\alpha, z_0)$ is that it depends not only on the distance z_0 but also on the polar orientation α of the emission dipole of the fluorescent molecule. We checked by polarization-resolved fluorescence imaging on GUVs that the fluorescent dyes are randomly oriented with respect to the bilayer (Figure 3 and 4); due to flexibility of the linker with which the dye is attached to the peptide we assume that the dye undergoes rotational diffusion on a time scale that is much faster than its fluorescence lifetime. In that case, the emission power $S_0(\alpha, z_0)$ in Equation (1) can be replaced by its value averaged over angle α, that is, by the expression:

$$S(z_0) = \frac{1}{3}S_\perp(z_0) + \frac{2}{3}S_\parallel(z_0),$$

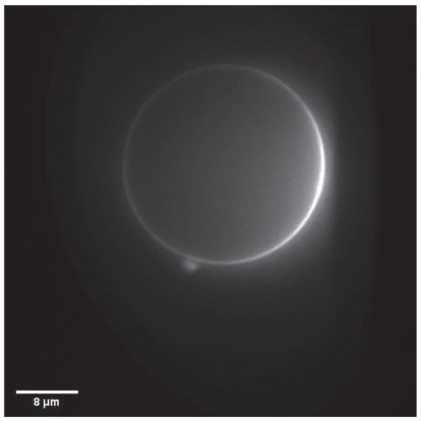

FIGURE 3 A giant unilamellar vesicle (GUV) image was achieved by using linear polarized excitation, which supports the assumption that the dye is oriented randomly

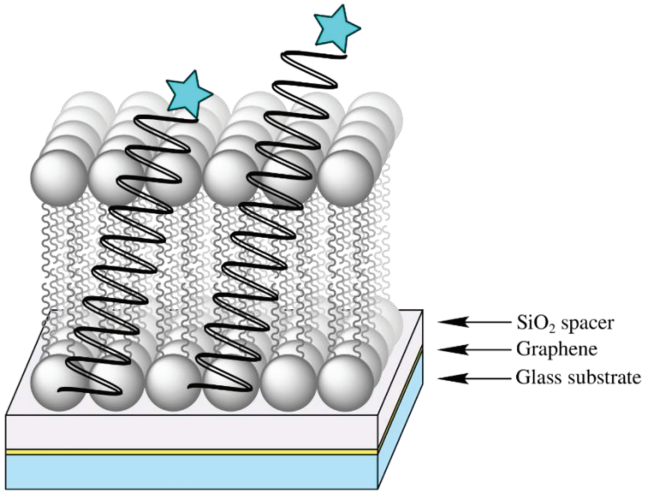

FIGURE 4 Schematic overview of the metal-induced energy transfer (MIET) measurements performed: giant unilamellar vesicles (GUVs) consisting of atto-labeled peptides (blue star) and DOPC were distributed on a graphene layer embedded between a SiO_2 spacer (10 nm) and a glass substrate. Fluorescence lifetime decay curves were measured, and the respective heights with respect to the graphene layer were determined using the graphene-induced energy transfer (GIET) curve

where $S_{\perp}(z_0)$ and $S_{\parallel}(z_0)$ are the distance-dependent emission powers for dipoles oriented perpendicularly and parallel to the substrate surface, respectively. The finally calculated distance-dependent lifetime curve (metal-induced energy transfer [MIET] curve) $\tau(z_0)$ for the specific sample configuration and dye used in our experiments is shown in Section 3 (Figure 5).

3 | RESULTS AND DISCUSSION

The peptide sequence for the membrane-bound molecular ruler was chosen following previous studies that implemented β-peptides as

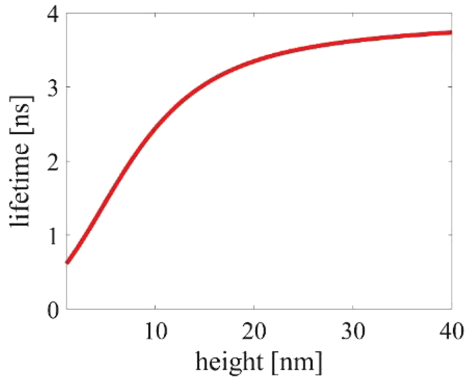

FIGURE 5 Calculated graphene-induced energy transfer (GIET) curve for the dipole random orientation. The calculation considers the 10-nm thickness of the SiO_2 layer on top of the graphene surface, which is deposited to prevent complete fluorescence quenching

transmembrane helices.[19] The hydrophobic portion consists of 19 consecutive β^3-D-homovaline amino acids flanked by two β^3-D-homotryptophan and two β^3-D-homolysine units on each side of the peptide. In general, charged amino acids enhance the peptide solubility in aqueous media, whereas tryptophan is known to promote peptid anchoring within the lipid headgroup area.[31–35] Heavy-atom-labeled X-ray studies demonstrated that such a β-peptide model system is successfully incorporated spanning the lipid membranes. The transmembrane peptide 14-helices are tilted about 16° in the positive hydrophobic mismatch situation to match the membrane thickness of DOPC.[19] To investigate the membrane-proximal environment at different heights with respect to the lower leaflet, two different transmembrane domains were synthesized. Peptide **P1** models the immediate membrane proximity by adding only β-alanine to the transmembrane domain and modifying it with the dye Atto643. In peptide **P2**, the transmembrane domain was elongated by six β-amino acids followed by β-alanine and Atto643 labeling. An alternating sequence of β^3-D-homovaline and β^3-D-homolysine was chosen for elongation because it improves solubility in aqueous environments while promoting 14-helix formation.[28] Using the 14-helix pitch of 5.0 Å derived from the literature and a tilt angle of 16°, the theoretical height of **P1** in DOPC is calculated to be 4.42 nm, whereas **P2** elongates to 5.36 nm.[17,19,36]

GIET was used to localize the fluorescent dye in fluorescently labeled peptides in an SLB. Atto643 peptide was incorporated at low concentration into a supported DOPC bilayer prepared on a graphene substrate. Fluorescence decay curves were acquired by scanning a 5 µm × 5 µm area with a custom-built confocal laser scanning microscope (CLSM; see Wegner et al.[22] for details) equipped with a 640-nm wavelength pulsed excitation laser, a single-photon avalanche photodiode detector, and high-speed electronics for time-correlated single-photon counting (TCSPC). The laser repetition rate was 20 MHz, the laser pulse width was ∼50 ps, and the temporal resolution of the TCSPC electronics was 16 ps. The total excitation power on the sample was 20 W, and the total scan time was 400 ms for each image, which consisted of 200 × 200 pixels. The measurements were

repeated three times in three different sample areas to obtain sufficiently good lifetime data. The standard deviations of the lifetime and height values were obtained by using three such independent measurements. The recorded TCSPC lifetime histograms were fitted with a triple exponential decay function using a maximum likelihood estimator, with the third component fixed to the free-space lifetime of the dye in solution. Using the GIET curve shown in Figure 5, the lifetime values were converted to distance values. To calculate the GIET curve, we needed to know the free-space lifetime and QY of the dye while bound to the peptide. The free-space lifetime of the dye-peptide construct in solution was determined by an independent TCSPC measurement at 4 ns. By comparing this value with the known lifetime (3.5 ns) and QY (0.62) of the pure dye, and assuming that lifetime and QY are inversely proportional, we determined the QY value of peptide-Atto 643 to be 0.71. In calculating the GIET curve, we also took into account the presence of the bilayer, which was assumed to have a refractive index of 1.46 and a thickness of ~5 nm. The thickness of the graphene layer was set to 0.34 nm and its complex-valued refractive index to $2.77 + 1.42i$ for the maximum fluorescence emission wavelength of 690 nm. The refractive index of the 10-nm-thick silicon dioxide layer deposited on the graphene layer was set to 1.46.

In Figure 5, the calculated GIET curve is shown that was used to convert the experimental lifetime values into spacing values, and Figure 6 shows the measured and fitted fluorescence decay curves for the two peptide samples. Using the GIET curve, we converted the measured fluorescence decay times into distance values and found the following values for axial dye distances. For the **P1** transmembrane peptide in a supported DOPC bilayer, we find dye spacings of 2.9 ± 0.3 and 8.4 ± 0.1 nm, corresponding to the two possible positions below and above the bilayer. For the **P2** transmembrane peptide, we find values of 1.70 ± 0.03 and 7.90 ± 0.27 nm, again for the two possible configurations of the dye below and above the DOPC bilayer. The different distance values for the bottom-oriented dyes are probably caused by the different lengths of **P1** and **P2**.

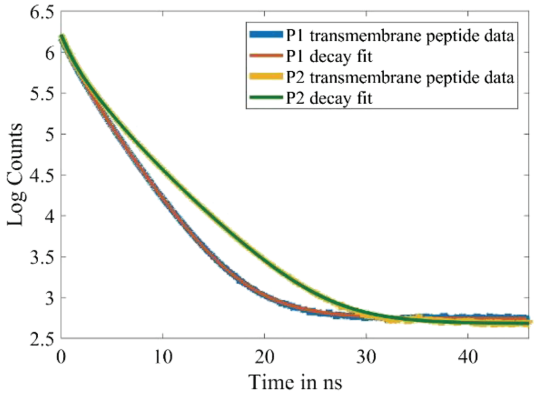

FIGURE 6 Fluorescence lifetime decay curve (blue and yellow) was tail-fitted with a three-exponential function using MLE, with a cutoff of 0.3 ns. The fitted curve is shown in red and pink for **P1** and **P2** transmembrane peptide, respectively. The third component is considered for the free dye in the solution

However, it is not fully clear how such a distance arises with both fluorophores being attached *N*-terminally in both cases. From these data, one can calculate the axial distance between the dye positions below and above the bilayer of 5.5 ± 0.4 nm for **P1** and of 6.2 ± 0.2 nm for **P2**. These values agree well with those found for the axial interdye distance of 5.5 ± 0.2 in head group-labeled DOPC bilayers, as reported in Appella et al.[24] Assuming a peptide tilt angle of 16°, the theoretically expected values for **P1** and **P2** are 4.44 and 5.36 nm, respectively. Our measurements give slightly larger values due to the additional linker and dye size, but they are in excellent agreement with these theoretical estimates. This also indicates that the **P2** peptide retains its rigidity when incorporated into the DOPC bilayer.

4 | CONCLUSION

An approach was presented to use β-peptide helices as molecular rulers to determine the distance to the membrane surface and to place probes at defined distances from the membrane surface. In the long term, these probes will provide the ability to determine the proton or calcium ion gradient along the membrane as a function of distance from the membrane head groups.

The molecular ruler is based on the conformational rigidity and helical persistence of a β-peptide 14-helix in combination with the knowledge to anchor the β-peptide as a transmembrane domain in a well-defined manner with respect to mobility and tilt angle. Furthermore, helical persistence within the outer membrane region is important for this approach as well as the possibility to functionalize the helix at defined positions with fluorophores or probes. In follow-up studies, it will therefore be important to further stabilize the transmembrane-extending 14-helix peptide conformation by engineering features such as ACHC or salt bridges. General proof of concept was performed with an *N*-terminally attached Atto643 fluorophore to determine the heights of the fluorophore relative to the lower leaflet of the MIET membrane. After spreading GUVs on a graphene-coated glass substrate, GIET spectroscopy was performed to determine the heights of the fluorophores of the respective TMDs being in agreement with the predicted values.

ACKNOWLEDGEMENTS

Generous support from the Deutsche Forschungsgemeinschaft (DFG; SFB 803, Project A01) is gratefully acknowledged. JE acknowledges support by the DFG (German Research Foundation) under Germany's Excellence Strategy—EXC 2067/1-390729940.

Open Access funding enabled and organized by Projekt DEAL.

ORCID

Jörg Enderlein https://orcid.org/0000-0001-5091-7157
Ulf Diederichsen https://orcid.org/0000-0002-2654-9160

REFERENCES

1. Joseph B, Sikora A, Bordignon E, Jeschke G, Cafiso DS, Prisner TF. Distance measurement on an endogenous membrane transporter in

E. coli cells and native membranes using EPR spectroscopy. *Angew Chem Int Ed*. 2015;54(21):6196-6199. https://doi.org/10.1002/anie.201501086
2. Gandhi A, Lakshminarasimhan D, Sun Y, Guo H-C. Structural Insights into the molecular ruler mechanism of the endoplasmic reticulum aminopeptidase ERAP1. *Sci Rep*. 2011;1(1):186. https://doi.org/10.1038/srep00186
3. Eberhard H, Diezmann F, Seitz O. DNA as a molecular ruler: interrogation of a tandem SH2 domain with self-assembled, bivalent DNA-peptide complexes. *Angew Chem*. 2011;123(18):4232-4236. https://doi.org/10.1002/ange.201007593
4. Abendroth F, Bujotzek A, Shan M, Haag R, Weber M, Seitz O. DNA-controlled bivalent presentation of ligands for the estrogen receptor. *Angew Chem Int Ed*. 2011;50(37):8592-8596. https://doi.org/10.1002/anie.201101655
5. Zettl T, Mathew RS, Seifert S, Doniach S, Harbury PAB, Lipfert J. Absolute intramolecular distance measurements with angstrom-resolution using anomalous small-angle X-ray scattering. *Nano Lett*. 2016;16(9):5353-5357. https://doi.org/10.1021/acs.nanolett.6b01160
6. Afri M, Alexenberg C, Aped P, et al. NMR-based molecular ruler for determining the depth of intercalants within the lipid bilayer. *Chem Phys Lipids*. 2014;184:105-118. https://doi.org/10.1016/j.chemphyslip.2014.07.007
7. Burns JR, Wood JW, Stulz E. A porphyrin-DNA chiroptical molecular ruler with base pair resolution. *Front Chem*. 2020;8:113. https://doi.org/10.3389/fchem.2020.00113
8. Littleton JT, Bai J, Vyas B, et al. Synaptotagmin mutants reveal essential functions for the C2B domain in Ca^{2+}-triggered fusion and recycling of synaptic vesicles in vivo. *J Neurosci*. 2001;21(5):1421-1433. https://doi.org/10.1523/JNEUROSCI.21-05-01421.2001
9. Anderson M, Moshnikova A, Engelman DM, Reshetnyak YK, Andreev OA. Probe for the measurement of cell surface pH in vivo and ex vivo. *Proc Natl Acad Sci*. 2016;113(29):8177-8181. https://doi.org/10.1073/pnas.1608247113
10. Carraretto L, Checchetto V, De Bortoli S, et al. Calcium flux across plant mitochondrial membranes: possible molecular players. *Front Plant Sci*. 2016;7. https://doi.org/10.3389/fpls.2016.00354
11. Sönnichsen C, Reinhard BM, Liphardt J, Alivisatos AP. A molecular ruler based on plasmon coupling of single gold and silver nanoparticles. *Nat Biotechnol*. 2005;23(6):741-745. https://doi.org/10.1038/nbt1100
12. Mathew-Fenn RS, Das R, Silverman JA, Walker PA, Harbury PAB. A molecular ruler for measuring quantitative distance distributions. *PLoS ONE*. 2008;3(10):e3229. https://doi.org/10.1371/journal.pone.0003229
13. Frackenpohl J, Arvidsson PI, Schreiber JV, Seebach D. The outstanding biological stability of beta- and gamma-peptides toward proteolytic enzymes: an in vitro investigation with fifteen peptidases. *Chembiochem*. 2001;2(6):445-455. https://doi.org/10.1002/1439-7633(20010601)2:6%3C445::AID-CBIC445%3E3.3.CO;2-R
14. Cheng RP, Gellman SH, DeGrado WF. β-Peptides: from structure to function. *Chem Rev*. 2001;101(10):3219-3232. https://doi.org/10.1021/cr000045i
15. Seebach D, Gardiner J. β-Peptidic peptidomimetics. *Acc Chem Res*. 2008;41(10):1366-1375. https://doi.org/10.1021/ar700263g
16. Chakraborty P, Diederichsen U. Three-dimensional organization of helices: design principles for nucleobase-functionalized β-peptides. *Chemistry*. 2005;11(11):3207-3216. https://doi.org/10.1002/chem.200500004
17. Rost U, Steinem C, Diederichsen U. β-Glutamine-mediated self-association of transmembrane β-peptides within lipid bilayers. *Chem Sci*. 2016;7(9):5900-5907. https://doi.org/10.1039/C6SC01147K
18. Pahlke DM, Diederichsen U. Synthesis and characterization of β-peptide helices as transmembrane domains in lipid model membranes: β-peptide transmembrane helices. *J Pept Sci*. 2016;22(10):636-641. https://doi.org/10.1002/psc.2912
19. Rost U, Xu Y, Salditt T, Diederichsen U. Heavy-atom labeled transmembrane β-peptides: synthesis, CD-spectroscopy, and X-ray diffraction studies in model lipid multilayer. *ChemPhysChem*. 2016;17(16):2525-2534. https://doi.org/10.1002/cphc.201600289
20. Brückner AM, Chakraborty P, Gellman SH, Diederichsen U. Molecular architecture with functionalized β-peptide helices. *Angew Chem Int Ed*. 2003;42(36):4395-4399. https://doi.org/10.1002/anie.200351871
21. Kabatas Glowacki S, Koszinowski K, Hübner D, Frauendorf H, Vana P, Diederichsen U. Supramolecular self-assembly of β^3-peptides mediated by Janus-type recognition units. *Chemistry*. 2020;26(53):12145-12149. https://doi.org/10.1002/chem.202003107
22. Wegner J, Valora G, Halbmair K, et al. Semi-rigid nitroxide spin label for long-range EPR distance measurements of lipid bilayer embedded β-peptides. *Chemistry*. 2019;25(9):2203-2207. https://doi.org/10.1002/chem.201805880
23. Tkach I, Diederichsen U, Bennati M. Studies of transmembrane peptides by pulse dipolar spectroscopy with semi-rigid TOPP spin labels. *Eur Biophys J*. 2021;50(2):143-157. https://doi.org/10.1007/s00249-021-01508-6
24. Appella DH, Barchi JJ, Durell SR, Gellman SH. Formation of short, stable helices in aqueous solution by β-amino acid hexamers. *J Am Chem Soc*. 1999;121(10):2309-2310. https://doi.org/10.1021/ja983918n
25. Raguse TL, Porter EA, Weisblum B, Gellman SH. Structure-activity studies of 14-helical antimicrobial beta-peptides: probing the relationship between conformational stability and antimicrobial potency. *J am Chem Soc*. 2002;124(43):12774-12785. https://doi.org/10.1021/ja0270423
26. Cheng RP, DeGrado WF. De novo design of a monomeric helical β-peptide stabilized by electrostatic interactions. *J am Chem Soc*. 2001;123(21):5162-5163. https://doi.org/10.1021/ja010438e
27. Arvidsson PI, Rueping M, Seebach D. Design, machine synthesis, and NMR-solution structure of a β-heptapeptide forming a salt-bridge stabilised 3_{14}-helix in methanol and in water. *Chem Comm*. 2001;7:649-650. https://doi.org/10.1039/B101085I
28. Pahlke DM. Synthesis, characterization and sensor-functionalization of transmembrane β-peptides, Dissertation, Göttingen 2018.
29. Ghosh A, Sharma A, Chizhik AI, et al. Graphene-based metal-induced energy transfer for sub-nanometre optical localization. *Nat Photonics*. 2019;13(12):860-865. https://doi.org/10.1038/s41566-019-0510-7
30. Moerland RJ, Hoogenboom JP. Subnanometer-accuracy optical distance ruler based on fluorescence quenching by transparent conductors. *Optica*. 2016;3(2):112-117. https://doi.org/10.1364/OPTICA.3.000112
31. de Planque MRR, Bonev BB, Demmers JAA, et al. Interfacial anchor properties of tryptophan residues in transmembrane peptides can dominate over hydrophobic matching effects in peptide-lipid interactions. *Biochemistry*. 2003;42(18):5341-5348. https://doi.org/10.1021/bi027000r
32. Killian JA, von Heijne G. How proteins adapt to a membrane-water interface. *Trends Biochem Sci*. 2000;25(9):429-434. https://doi.org/10.1016/s0968-0004(00)01626-1
33. Wiefel L, Steinbüchel A. Solubility behavior of cyanophycin depending on lysine content. *Appl Environ Microbiol*. 2014;80(3):1091-1096. https://doi.org/10.1128/AEM.03159-13
34. de Planque MRR, Kruijtzer JAW, Liskamp RMJ, et al. Different membrane anchoring positions of tryptophan and lysine in synthetic

transmembrane α-helical peptides. *J Biol Chem*. 1999;274(30):20839-20846. https://doi.org/10.1074/jbc.274.30.20839

35. Wimley WC, White SH. Membrane partitioning: distinguishing bilayer effects from the hydrophobic effect. *Biochemistry*. 1993;32(25):6307-6312. https://doi.org/10.1021/bi00076a001
36. Seebach D, Matthews JL. β-Peptides: a surprise at every turn. *Chem Commun*. 1997;21(21):2015-2022. https://doi.org/10.1039/a704933a

How to cite this article: Kloos M, Sharma A, Enderlein J, Diederichsen U. Transmembrane β-peptide helices as molecular rulers at the membrane surface. *J Pep Sci*. 2021;27(11):e3355. https://doi.org/10.1002/psc.3355